Modern Physics Letters B, Vol. 22, No. 13 (2008) 1273–1295

World Scientific
www.worldscientific.com

INTERMEDIATE VALENCE METALS

JON LAWRENCE
Department of Physics and Astronomy, University of California, Irvine, California 92697, USA

Received 13 March 2008

The ground state of rare earth intermediate valence (IV) metals is that of a heavy mass Fermi liquid. The transport, optical conductivity, dHvA signals, and Q-resolved neutron spectra reflect the existence of a Fermi surface with strongly renormalized masses and a hybridization gap. On the other hand, properties such as the susceptibility, specific heat, valence and spin dynamics that are dominated by the spin fluctuations, which are highly localized, can be understood qualitatively (and sometimes quantitatively) as those of a collection of non-interacting Anderson/Kondo impurities. Anomalies exist in some compounds both in the low temperature behavior and in the rate of crossover from Fermi liquid to local moment behavior which may reflect non-universal behavior of the Anderson lattice.

Keywords: Intermediate valence; heavy fermions; correlated electrons.

The rare earth intermediate valence (IV) behavior which occurs in many cerium and ytterbium compounds presents an archetypal example of correlated electron behavior.[1–3] The IV metals are related to the heavy Fermion (HF) compounds.[4] The underlying physics in both cases is that of highly localized $4f$ orbitals weakly hybridizing with conduction electrons in the presence of a strong on-site Coulomb interaction between the $4f$ orbitals, which inhibits itineracy by preventing multiple occupancy of the orbital. The result is often a paramagnetic Fermi liquid ground state where the $4f$ orbitals contribute to a quasiparticle band that is characterized by a large effective mass m^*.

While the basic physics — correlated hopping on and off the $4f$ orbitals — is the same as in the heavy Fermions, the latter typically have effective masses in the range $m^* \sim$ 100–1000 $\mathrm{m_e}$, while the IV compounds are "moderately heavy Fermions" with $m^* \sim$ 10–50 $\mathrm{m_e}$. The very large masses of the HF compounds are associated with proximity to a quantum critical point[5] (QCP) for a transition between a paramagnetic Fermi liquid state and a magnetic state, typically antiferromagnetic (AF), where the $4f$ electrons are essentially localized. Fluctuations into the AF state are present in the paramagnetic state, and have a strong effect on the bulk properties, often leading to "non-Fermi Liquid" (NFL) behavior. On the other hand, the IV compounds are not close to a QCP and show no signs of AF correlations.

Instead, they exhibit larger $4f$/conduction hybridization, and have many properties in common with the so-called Kondo insulators.[6] In the Kondo insulators, the $4f$/conduction electron level crossing leads to a hybridization gap with the Fermi level in the gap. There is considerable evidence that a hybridization gap exists in the IV metals, with the Fermi level in a region of high density of states near the gap edge.

The heavy Fermions exhibit several possible ground states, namely heavy Fermi liquids, marginal Fermi liquids (i.e. NFL behavior), heavy mass superconductivity, and small moment magnetism. The IV compounds are either moderately heavy mass Fermi liquids, as in $CePd_3$, $YbAl_3$, $YbAgCu_4$, or Kondo insulators as in $Ce_3Bi_4Pt_3$ and YbB_{12}. In some compounds, such as elemental cerium metal or $YbInCu_4$, there are also first-order valence transitions, where there is a significant change in hybridization, effective mass, and Kondo temperature, with no concomitant change in crystal symmetry.

The HF compounds typically have low crystal symmetries (tetragonal, hexagonal or orthorhombic) leading to significant anisotropy (indeed, in some cases, to quasi 2D behavior) and to crystal field splitting. In particular, the spin decay rate, as measured by the characteristic energy for spin fluctuations (the so-called Kondo temperature T_K that is inversely proportional to m^*) satisfies $k_BT_K/\hbar \sim 10$ K $< k_BT_{cf}/\hbar \sim 100$ K, where k_BT_{cf} is the crystal field splitting. This means that the heavy fermion behavior arises from a ground state multiplet, which is typically a doublet. On the other hand, the IV compounds mostly have cubic symmetry (e.g. fcc, Cu_3Au, C15B), and the associated spin decay rate is large $k_BT_K/\hbar \sim 500$ K $> k_BT_{cf}/\hbar$. Under these circumstances, the ground multiplet has the full $N_J = 2J+1$ degeneracy of the $4f$ spin-orbit coupled local moment ($N_J = 6$ for $J = 5/2$ cerium and 8 for $J = 7/2$ ytterbium).

We thus see that the correlated electron problem in the IV metals has a great deal of simplicity relative to the HF compounds: nearly isotropic 3D behavior, no complications due to crystal fields or antiferromagnetic correlations, and a large orbital degeneracy (which allows for simplifying theoretical approximations). The hybridization gap seems to play a crucial role. The situation is more complex than that of the transition metals (e.g. Pd) where a one-band Hubbard Model in three dimensions (3D) is appropriate, but less complex than the transition metal oxides (e.g. the high-T_c cuprates) which have multiple bands, 2D character, possible hidden order, and a possible quantum critical point.

While IV behavior occurs in compounds of a number of rare earths, including Eu, Sm and Tm compounds, and is often associated with Kondo insulator behavior, in what follows I will focus on a number of classic Ce and Yb compounds ($CeBe_{13}$, $CePd_3$, $CeSn_3$, $YbAl_3$ and $YbXCu_4$) where metallic, Fermi liquid ground states occur. I will also restrict attention to a small number of key measurements — bulk measurements such as susceptibility, specific heat, resistivity, and spectroscopic measurements such as photoemission, de Haas van Alphen, optical conductivity,

and neutron scattering — chosen to best illuminate the basic IV behavior, with an emphasis on measurements on high quality single crystals. (I will not discuss the valence transitions and other effects that arise from strong coupling of the valence fluctuations to the lattice.)

The term intermediate valence refers to non-integral valence, which corresponds to fractional occupation of the $4f$ shell, with the remaining fraction of electrons transferred into the conduction band. This occurs when two integral valence states are nearly degenerate in energy. For Ce, the relevant states are $(5d6s)^3 4f^1$ and $(5d6s)^4 4f^0$. For these configurations, the $4f$ occupation number is $n_f = 1, 0$ and the atom is trivalent, tetravalent, respectively. For Yb, the states are $(5d6s)^3\ 4f^{13}$ and $(5d6s)^2\ 4f^{14}$; defining the $4f$ occupation number as the number of *holes* in the otherwise full $4f^{14}$ shell, these configurations have $n_f = 1, 0$ and are trivalent, divalent respectively. Other states, such as $(5d6s)^2 4f^2$ for Ce or $4f^{12}(5d6s)^4$ for Yb, are at very high energy due to the on-site Coulomb interaction.

In an (oversimplified) single ion model, intermediate valence occurs when the two nearly-degenerate localized configurations form a hybridized wave function; e.g.

$$a[4f^1(5d6s)^3\rangle + b[4f^0(5d6s)^4\rangle\,, \tag{1}$$

where $a = \sqrt{n_f}$ and $b = \sqrt{(1 - n_f)}$ and where n_f here is the *average* $4f$ occupancy. The valence (or number of outer shell conduction electrons contributing to the bonding) is then $z = 4 - n_f$ for Ce and $2 + n_f$ for Yb. For IV $CePd_3$, where $n_f = 0.8$ ($z = 3.2$), we can write the resulting configuration as $(5d6s)^{3.2} 4f^{0.8}$. Similarly, for IV $YbAl_3$ where $n_f = 0.75$ ($z = 2.75$), the configuration is $(5d6s)^{2.75}$ $4f^{13.25}$. In an actual periodic IV metal, these ionic states can be viewed as forming local states from which the band states are derived.

The basic behavior of Yb and Ce IV intermetallic compounds is as follows. In the high temperature limit, the rare earth approaches integral valence with $n_f \to 1$. This is the trivalent configuration for both Ce and Yb. The material is then a local moment paramagnet, obeying a Curie law $\chi \to C_J/T$ where the Curie constant is $C_J = Ng^2\mu_B^2 J(J+1)/3k_B$; the entropy approaches $R\ln(2J+1)$. At a characteristic temperature T_0 there is a crossover to the low temperature limit, where the behavior is that of a Fermi liquid. In this limit, the valence is non-integral ($n_f < 1$) and the system behaves as a Pauli paramagnet, with a T-linear specific heat $C_v \sim \gamma T$.

In a non-interacting Fermi gas, the Pauli susceptibility and the linear coefficient of specific heat are proportional to $N(\varepsilon_F)$, the density of states (DOS) at the Fermi energy, which for parabolic bands is proportional to the electron mass m_e. Fermi liquids are metals where, despite strong electron-electron interactions, the statistics at low T are those of a free (non-interacting) Fermi gas, but with the replacement $m \to m^*$ (the *effective mass*). For a simple metal such as potassium, $\gamma = 2$ mJ/mol-K^2 and $m^* = 1.25\ m_e$. An IV compound is a heavy Fermi liquid, with a large effective mass reflecting the correlated hybridization of the local $4f$ states into the conduction electrons. The resulting large DOS leads to an enhanced Pauli susceptibility and a large specific heat coefficient. The effective masses derived

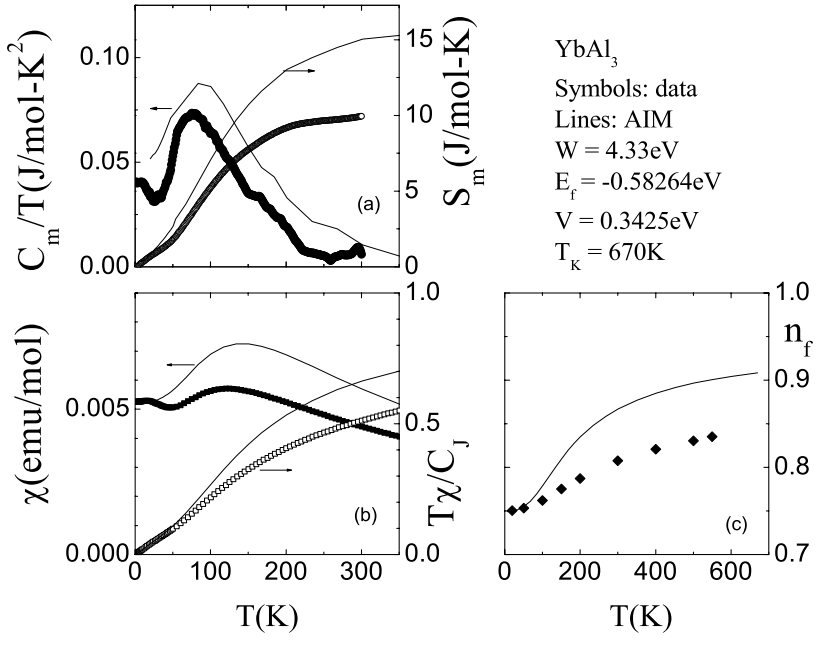

Fig. 1. Comparison of the experimental behavior (symbols) of $YbAl_3$ to the predictions of the Anderson impurity model (lines). (The parameters of the model are given above panel (c).) (a) The magnetic contribution C_m to the specific heat, plotted as C_m/T (solid symbols), and the corresponding entropy (open symbols). (b) The susceptibility χ (solid symbols) and corresponding "effective moment" $T\chi/C_J$ (open symbols) where C_J is the Curie constant. (c) The $4f$ occupation number, measured by L_3 X-ray absorption. (Adapted with permission from Ref. 7, Copyright 2002, American Physical Society.)

from the specific heat and susceptibility also are found to vary inversely with the crossover temperature, i.e. $\gamma, \chi(0) \sim 1/T_0$.

As an example, we consider the compound $YbAl_3$ (Fig. 1).[7] As mentioned, the ground state valence is 2.75 ($n_f = 0.75$). (The $4f$ occupation number is obtained by a standard analysis[8] of the L_3 X-ray absorption edge.) The low temperature susceptibility is constant at the value $\chi(0) = 0.0052$ emu/mol and the linear coefficient of specific heat is $\gamma_m = 40$ mJ/mol-K^2 with corresponding effective mass $m^* = 25$ m$_e$. This is "moderately heavy fermion" behavior. The general features of Fig. 1 — Curie behavior of the susceptibility at high temperature, with a broad peak in the range 100–200 K and a finite value at low temperature; a smooth evolution of the $4f$ occupation number towards $n_f = 1$ over a comparable temperature scale; and an enhanced linear coefficient of specific heat in the range $\gamma \sim 50$–100 mJ/mol-K^2 — are observed in almost all metallic IV compounds.

Since the absorption of the $(2J + 1)$ spin degrees of freedom into the heavy $4f$ bands at low temperature, and the associated generation of $R\ln(2J+1)$ entropy over the scale T_0 gives rise to the large specific heat and the enhanced Pauli susceptibility, the spin fluctuation spectra of these compounds carries essential information about

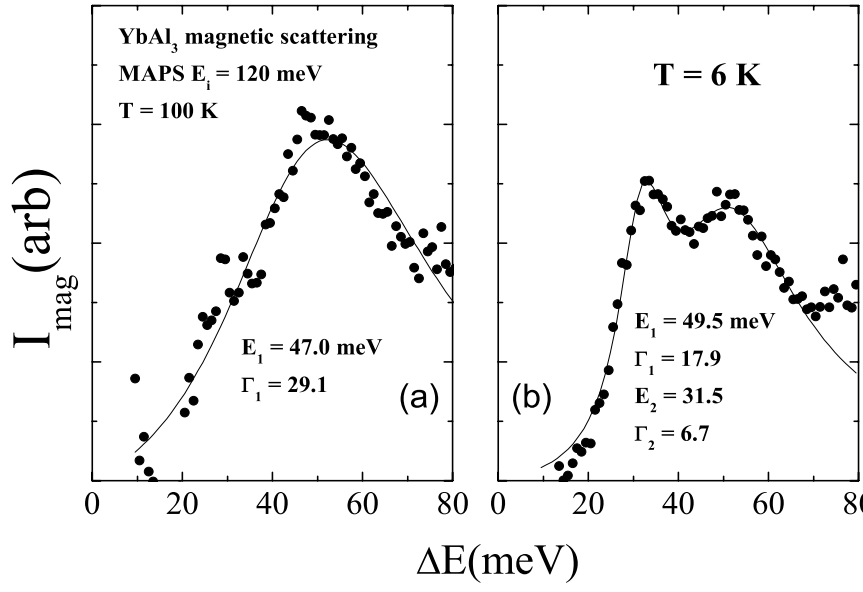

Fig. 2. Polycrystalline-averaged inelastic magnetic neutron scattering spectra for data taken on $YbAl_3$ using the MAPS spectrometer at ISIS, Rutherford-Appleton Laboratory. (a) 100 K and (b) 6 K. The lines are Lorentzian fits, with parameters given in the panels.

the IV state. Typically, the spin dynamics show a Lorentzian power spectrum

$$\begin{aligned} \chi''(Q,E) &= (n(E)+1)f^2(Q)\chi'(Q)E\,P(E)\,, \\ P(E) &= (\Gamma/2)/\{(E-E_0)^2+\Gamma^2)\}\,, \end{aligned} \tag{2}$$

where $f^2(Q)$ is the $4f$ form factor and $(n(E)+1)$ is the (Bose) thermal factor. Many neutron studies of polycrystalline samples[9] where the Q-dependence is averaged out show that at high temperatures the scattering is quasielastic ($E_0 = 0$) with linewidth Γ related to the crossover temperature via $\Gamma \sim k_B T_0$. At low temperatures, the scattering becomes inelastic, with E_0 and Γ both of order $k_B T_0$. This can be seen for $YbAl_3$ at 100 K in Fig. 2(a). (At lower temperature, there is an additional peak, which will be discussed further below.) Only a small number of neutron scattering experiments have been performed on single crystal IV compounds where the Q-dependence can be determined. In $YbInCu_4$ it was found[10] that the scattering at five Q in the Brillouin zone (BZ) showed no dependence of Γ or E_0 on Q and only a weak (15%) dependence of χ' on Q. Such a Q-independent, broad Lorentzian response implies that the primary excitation is a local, highly damped spin fluctuation (oscillation) at characteristic energy $E_0 = k_B T_0$.

These properties of IV compounds are captured by the Anderson Impurity Model (AIM),[11,12] in which an f-atom resides at the origin and hybridizes with a background conduction band. The parameters of the model are as follows. An energy E_f is required to promote the magnetic $n_f = 1$ state to the nonmagnetic $n_f = 0$ state. A strong on-site Coulomb interaction raises the energy of the $n_f = 2$

state by an amount U above the $n_f = 1$ state. The matrix element V_{kf} measures the amplitude of hybridization of the f orbitals with the conduction electron k-states. The resulting hybridization strength for the conduction electrons to hop on and off the f orbital is $\Delta = V_{kf}^2 \rho(\varepsilon_F)$, where $\rho(\varepsilon_F)$ is the density of *conduction* states at the Fermi level ε_F. Typically for the rare earths, $\Gamma \sim 0.1$ eV, $E_f \sim 1$ eV and $U \sim 10$ eV. The large on-site Coulomb interaction suppresses hopping into the $n_f = 2$ state, so that if the instantaneous state is $n_f = 1$, then the electron can hop off, but not on, to the f orbital. The result is a classic correlated electron problem: because the $n_f = 2$ occupation is suppressed, motion in and out of the f orbital is slowed down from the bare rate Δ/h to a renormalized rate $k_B T_K/h$, where T_K is the Kondo temperature, which satisfies

$$k_B T_K \sim \varepsilon_F \exp\{-E_f/(N_J \Delta)\} . \tag{3}$$

It can be seen that when $N_J \Delta \ll E_f$, there is an exponential suppression of the hopping rate. Low energy spin fluctuations then arise from such virtual charge fluctuations as $(n_f = 1, \uparrow) \rightarrow n_f = 0 \rightarrow (n_f = 1, \downarrow)$. These in turn create a narrow $4f$ resonance at the Fermi level ε_F, known as the "Kondo resonance."

The AIM predicts that at high temperature, spin entropy dominates hybridization, so that integral valence ($n_f = 1$) and local moment behavior (Curie law and $R \ln(2J+1)$ entropy) occurs. There is a crossover, on the scale of T_K, to a low temperature "local Fermi liquid" state, where the hybridization results in the Kondo resonance, which in turn causes an f contribution to the density-of-states (DOS) of order $N_f(\varepsilon_F) \sim 1/k_B T_K$. Hence the specific heat coefficient γ and Pauli susceptibility $\chi(0)$ are enhanced by an amount of order $1/T_K$. The valence is non-integral ($n_f < 1$) and the energy of the system is lowered by an amount $k_B T_K$, which in the "Kondo limit" (when n_f is only a little smaller than unity) can be expressed as

$$k_B T_K \sim N_J \tilde{V}^2 \rho(\varepsilon_F) , \tag{4}$$

where the renormalized hybridization is given by

$$\tilde{V}^2 = (1 - n_f) V^2 . \tag{5}$$

The factor $(1 - n_f)$ reflects the correlations due to large U. In addition, the dynamics of the f spin fluctuations are those of a localized, damped oscillator with characteristic energy $E_0 = k_B T_K$ with $\chi'' \sim \chi(T) E\Gamma/((E - E_0)^2 + \Gamma^2)$. A very important aspect of the model is *universality*: properties such as the specific heat $C(T)$, susceptibility $\chi(T)$ and spin dynamics spectra $\chi''(E)$ scale as T/T_K, $E/k_B T_K$ and $\mu_B H/k_B T_K$. In the Kondo limit, for example, this leads to a universal Wilson ratio $(\pi^2 R/3C_J)\chi(0)/\gamma \cong 1 + (1/2J)$ which depends only on the orbital degeneracy N_J.

To show how well the AIM describes the data of IV metals, we consider two cases: $YbAgCu_4$ and $YbAl_3$.[7,8] For the theoretical predictions, we used code for an IV Anderson impurity in the non-crossing approximation (NCA) which essentially involves a $1/N_J$ expansion, appropriate for the large orbital degeneracy ($N_J = 8$)

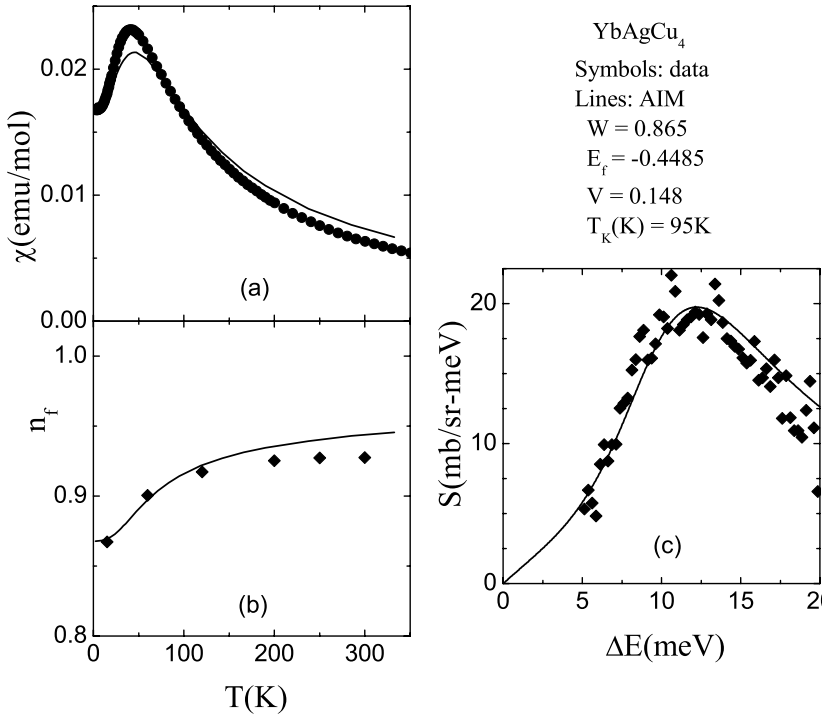

Fig. 3. Comparison of the experimental behavior (symbols) of $YbAgCu_4$ to the predictions of the Anderson impurity model (lines). (The parameters of the model are given above panel (c).) (a) Susceptibility, (b) $4f$ occupation number, (c) polycrystalline-averaged inelastic magnetic neutron scattering. (Adapted with permission from Ref. 8, Copyright 2001, American Physical Society.)

of Yb. Fitting the data requires the choice of three parameters: the hybridization amplitude V, the excitation energy E_f, and the background conduction band width W. We obtain the latter from the specific heat coefficient of the nonmagnetic counterpart compounds $LuAl_3$ and $LuAgCu_4$. (For many experimental techniques, the La (Lu) counterpart compound to a given Ce (Yb) compound is assumed to capture the physics of non-magnetic background, so that the difference is due entirely to the $4f$ contribution.) Given W, the latter two parameters are fixed by two measurements, e.g. the $T = 0$ values of the $4f$ occupation number $n_f(0)$ and the susceptibility $\chi(0)$. The Kondo temperature is then calculated from a formula similar to Eq. (3).

In Fig. 3, it can be seen that the AIM, with these three parameters as inputs, does an excellent quantitative job of reproducing the temperature dependence of the susceptibility and $4f$ occupation number, as well as the energy dependence of the (polycrystalline-averaged) inelastic magnetic neutron scattering spectrum of the IV compound $YbAgCu_4$, whose Kondo temperature is of the order 100 K. Similar good fits were observed for $YbTlCu_4$, which has a substantially larger Kondo

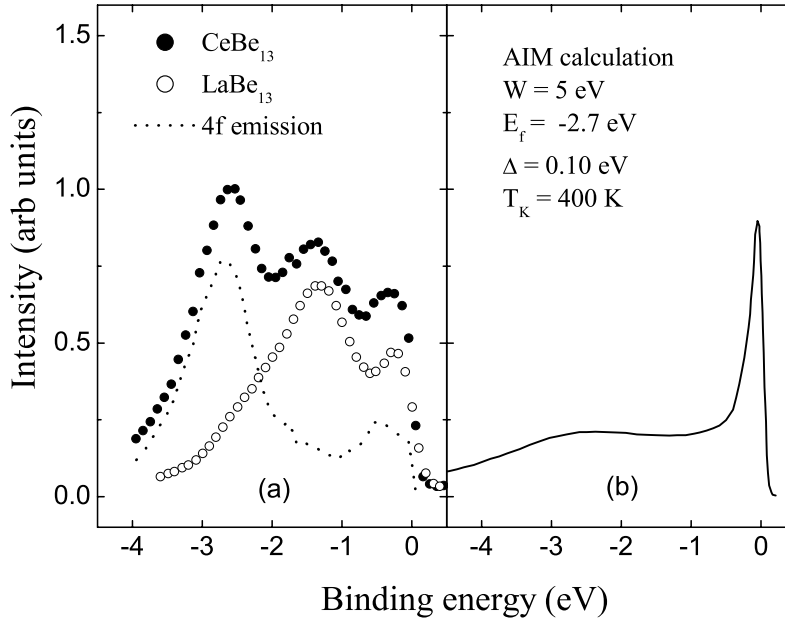

Fig. 4. (a) Ultraviolet photoemission spectra from polycrystalline specimens of $CeBe_{13}$ (solid circles) and $LaBe_{13}$ (open circles). The difference (dots), representing the $4f$ emission, consists of a Lorentzian peak centered at 2.7 eV binding energy, plus additional emission near the Fermi energy (zero binding energy). (b) Predictions of the Anderson impurity model (parameters given in panel (b) for the $4f$ emission. (Adapted with permission from Ref. 13, Copyright 1993, American Physical Society.)

temperature. For $YbAl_3$ (Fig. 1) the fits obtained from the $T = 0$ values of susceptibility and occupation number are semi-quantitative: the experimental data has the same qualitative features as the theory, and agrees in magnitude to 25%. For the inelastic neutron scattering, the AIM fit predicts that the dynamic susceptibility has the form of Eq. (2) with $E_0 = 40$ meV and $\Gamma = 22$ meV; it can be seen that at 100 K, the measured values are 47 and 29 mev respectively. Universality is further seen in the observed Wilson ratios, which are in the range 1–1.5 in most IV compounds, comparable to the AIM predictions.

The Kondo effect involves an exponential reduction of the energy scale $k_B T_K$ for spin fluctuations relative to the bare energies E_f, V, U and W. Photoemission experiments can measure the $4f^1 \rightarrow 4f^0$ excitation energy E_f as well as the bare hybridization width $\Delta = V^2 \rho(\varepsilon_F)$ and inverse photoemission, which measures the $4f_1 \rightarrow 4f^2$ transition, can be used to determine U. Comparison with the thermodynamic results, which are dominated by the low energy physics, would then show how well the AIM reproduces the relationship between large and small energy scales. In Fig. 4 we compare UPS data[13] for the IV compound $CeBe_{13}$ to the predictions of the AIM. Input parameters were W, E_f and Δ, chosen to reproduce the Kondo temperature (400 K) deduced from the susceptibility and neutron lineshape as well

as the measured $4f^1 \rightarrow 4f^0$ excitation energy; the hybridization width and valence are then predicted by the calculation. The data for $LaBe_{13}$ were subtracted to determine the $4f$ emission. The bare value $E_f = 2.7$ eV reproduces the main emission feature. The theory also predicts a peak near the Fermi energy in both photoemission and inverse photoemission that arises from the Kondo Resonance; the width of this feature should be proportional to T_K. The theory (Fig. 4(b)) clearly captures the qualitative features of the $4f$ emission (triangles in Fig. 4(a)) with peaks on both the bare scale E_f and on a smaller scale near the Fermi energy. While the fractional weight (28%) in the near-ε_F peak is well-reproduced by theory, the AIM appears to badly overestimate the linewidth of the $4f^1 \rightarrow 4f^0$ excitation.

Extensive work[14–16] on IV compounds in the 1980's and 1990's, primarily using polycrystalline or fractured single crystal samples, has clearly established the qualitative applicability of the Anderson impurity model to photoemission. Despite this, there is a long-standing argument about the degree to which the AIM relates the photoemission data to the bulk properties: whether the theory reproduces the measured weights, widths and positions of the main $4f^1 \rightarrow 4f^0$ and KR peaks, whether the temperature dependence is as predicted, and whether the bare energies are correctly related to the value of T_K obtained from bulk measurements. To a great extent, these problems arise from the high surface sensitivity of the measurement, coupled with the extreme structural and electronic reconstruction that can occur near the surface of rare earth IV compounds.

Although the AIM is intended for dilute alloys such as $La_{1-x}Ce_xPd_3$ for $x \ll 1$, we see that the impurity model gives a good qualitative (and sometimes surprisingly quantitative) description of the valence, specific heat, static and dynamic susceptibility of IV compounds, and this despite the fact that the $4f$ ions form a periodic array, and are far from the impurity limit. This is, I believe, essentially because these quantities are dominated by spin fluctuations, which are highly local in these materials.

The classic "Kondo effect" — a region of negative $d\rho/dT$ for the resistivity — is seen at high temperatures in some compounds such as $CePd_3$. For the low temperature transport behavior, however, the AIM fails badly. In particular, it predicts that the resistivity saturates to a finite value at $T = 0$ due to unitary scattering from the $4f$ impurity. However, when the $4f$ atoms form a periodic array, as in periodic IV metals, Bloch's law requires that the resistivity must vanish at $T = 0$. Typically in IV compounds the low temperature resistivity varies as $\rho \sim A(T/T_0)^2$. This quadratic temperature dependence is a sign of Fermi Liquid "coherence" among the spin fluctuations. In $YbAl_3$ this T^2 dependence occurs below the "coherence temperature" $T_{coh} \sim 40$ K (Fig. 5). Such quadratic temperature dependence is observed in all IV compounds; and it is found that the coefficient A is related in nearly-universal fashion to the square of the linear coefficient of specific heat through the "Kadowaki–Woods" ratio A/γ^2. This implies that $A \sim 1/T_K^2$, as expected on general grounds for electron-electron scattering in a band of width

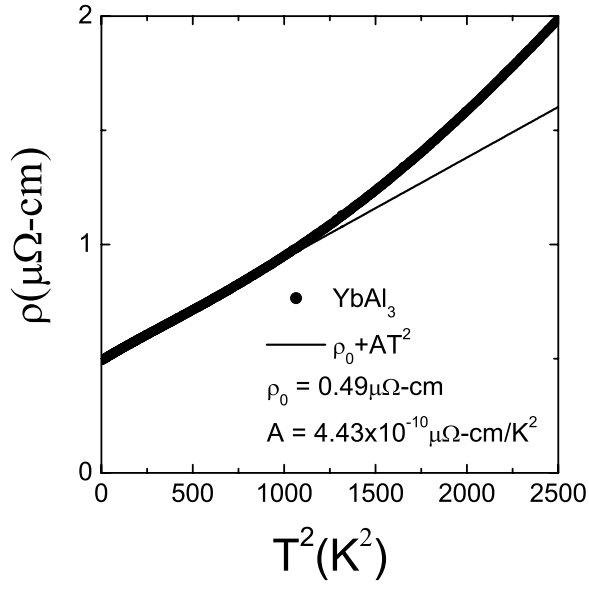

Fig. 5. Resistivity of $YbAl_3$, showing T^2 behavior for $T < T_{coh} \sim 40$ K. (Adapted with permission from Ref. 7, Copyright 2002, American Physical Society.)

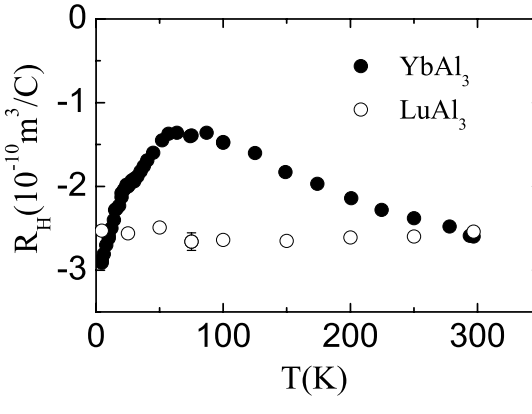

Fig. 6. Hall coefficient of $YbAl_3$ and $LuAl_3$, showing a rapid change for $T < T_{coh}$. (Adapted with permission from Ref. 7, Copyright 2002, American Physical Society.)

$k_B T_K$. It it has been established that this ratio depends on the orbital degeneracy $N_J = 2J + 1$.[17]

A rapid change is seen in the Hall coefficient of $YbAl_3$ in the same temperature range T_{coh} (Fig. 6). Since $R_H \sim 1/ne$ this suggests a change in carrier density, and hence in the Fermi surface, in the coherent ground state. Similar behavior of $R_H(T)$ is observed[18] in $CePd_3$ and $CeBe_{13}$, hence it appears to be a common feature of IV metals.

To get the correct transport behavior, including Bloch's law, and the coherent Fermi Liquid behavior, theory must treat the $4f$ *lattice*. There are two main theoretical approaches to accomplish this: band theory, where the $4f$ electrons are treated as itinerant, and the Anderson *lattice* model, which puts localized $4f$ electrons, with AIM interactions (E_f, V, U), on each site of a periodic lattice. Band theory, usually performed using the LDA (a spatially-smoothed density functional method) is designed to reproduce ground state properties, such as the Fermi surface geometry; it naturally includes hybridization but has difficulty including strong local correlations and temperature dependence. The Anderson lattice is complementary to band theory: it naturally includes correlations and temperature dependence, but cannot include details of the Fermi surface that arise due to band structure.

Direct measurement of the band structure can, in principle, be obtained from photoemission measurements. Since the $4f$ bands have large effective masses, and hence small dispersion, this requires energy resolution on the meV scale. While there has been enormous progress in HF/IV photoemission in recent years, in terms of resolution, high vacuum, flux, identification of the relative roles of surface and bulk emission etc., we are only very recently witnessing[19] the beginning of the level of sophistication (e.g. detailed Fermi surface mapping on surfaces whose structure in the near surface region is well-established) that has become routine for studies of the high temperature superconductors.

In the absence of very-high-resolution angle-resolved photoemission, the appropriate way to determine the renormalized Fermi surface of IV compounds is the de Haas van Alphen (dHvA) experiment. This requires samples of very low resistivity, and hence has only been attempted in a small number of cases. The dHvA experiment measures oscillations in the magnetization as a function of inverse magnetic field. The frequency of the oscillations is determined by the areas S of the extremal cross sections of the Fermi surface in the direction perpendicular to the applied field: $M = A\cos(2\pi F/H)$ where $F = (hc/2\pi e)S$. The temperature dependence of the amplitude determines the effective mass: $A = 1/\sinh(Qm^*T/H)$ where Q is a constant. In Fig. 7 it can be seen that the LDA correctly predicts the extremal areas of the Fermi surface for $YbAl_3$.[20] However, the same experiments show that band theory, which gives effective masses in the range $m^* \sim m_e$, strongly underestimates the effective masses which are measured to be in the range 15–25 m_e for the α, β and ε branches. For the IV compound $CeSn_3$,[21] the LDA also correctly predicts the Fermi surface topology and underestimates the masses. Because it does not treat the strong *local* Coulomb correlations accurately in the linearized density approximation, the LDA badly overestimates the band widths of the $4f$ electrons. The fact that it obtains the correct topology of the Fermi surface has long been recognized[22] as a consequence of Luttinger's theorem: the Fermi volume obtained for a non-interacting crystal is invariant when further electron-electron interactions are included.

The Anderson lattice (AL) model[12] extends the Anderson impurity model by having f-electron sites on a lattice. The model involves *level crossing* where a nar-

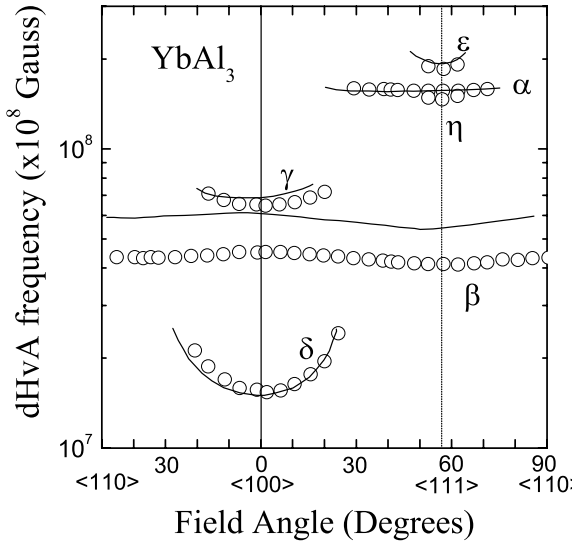

Fig. 7. Comparison of the measured de Haas van Alphen frequencies (symbols) of $YbAl_3$ to the predictions of the LDA (lines). (Adapted with permission from Ref. 20, Copyright 2000, Physical Society of Japan).

row $4f$ band at an energy E_f below the Fermi level ε_F is degenerate with and hybridizes (with matrix element V_{kf}) with a wide conduction band whose density of states is $\rho(E)$. In the absence of Coulomb correlations ($U = 0$) the hybridization and resulting level repulsion lead to a band structure with a hybridization gap of order $\Delta = N_J V^2 \rho$. As in the AIM, the Coulomb interaction U inhibits hopping when the site has the wrong occupation. This leads to an effective hybridization Hamiltonian with exponentially reduced renormalized parameters $\tilde{V} = (1-n_f)^{1/2} V$ and $U_{\text{eff}} \sim 0$. This effective Hamiltonian yields a coherent band structure with renormalized hybridized bands near the Fermi energy (Fig. 8). The bands exhibit a hybridization gap Δ_{eff} of order $\tilde{V}$ and an indirect gap of order T_K. In the IV metals, the Fermi level lies in the high DOS region due to the large admixture of $4f$ states. The large DOS is responsible for the large m^*. This renormalized band structure smoothly transforms back to the bare, unhybridized band structure with increasing temperature, resulting in a crossover from renormalized hybridized bands for $T \ll T_K$ to local moments uncoupled from band electrons for $T \gg T_K$.

The best evidence for the hybridization gap and its renormalization with temperature comes from optical conductivity measurements. At high temperature, the AL predicts normal Drude behavior due to scattering from local moments: $\sigma'(\omega) = (ne^2/m_b)\{\tau/(1+\tau^2\omega^2)\}$ where m_b is the bare band mass and τ is the relaxation time. There is a smooth crossover, on the scale T_K, to low temperature behavior where there is an IR absorption peak due to optical (vertical $Q = 0$) transitions across hybridization gap, plus a *very* narrow Drude peak due to low energy transitions right at the Fermi energy. In this Drude peak, both m_b and τ

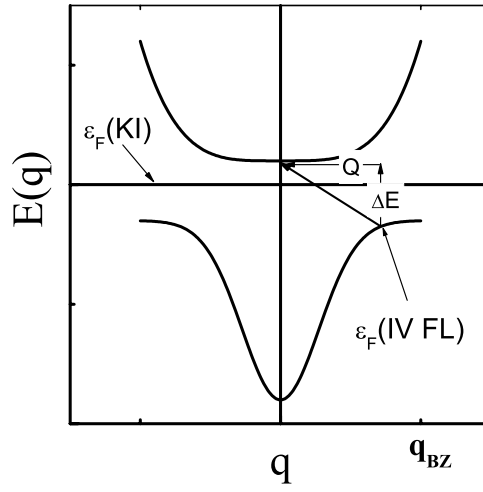

Fig. 8. Schematic renormalized band structure for the Anderson lattice. The level crossing of the $4f$ level with the conduction band leads to a hybridization gap. The Fermi level is in the gap for the Kondo insulators (KI), but is in a region of high density of states (DOS) for the IV metals (Fermi liquids FL). The arrows show a typical neutron excitation at well-defined energy transfer ΔE and momentum transfer Q. Transitions at Q equal the Brillouin zone vector q_{BZ} connect occupied and empty regions of high DOS. (Adapted with permission from Ref. 31, Copyright 2006, American Physical Society.)

are strongly renormalized:

$$\sigma'(\omega) = ne^2[\tau^*/m^*]\{1/(1+\tau^{*2}\omega^2)\} \tag{6}$$

where $m^* = \lambda m_b = m^*$ and $\tau^* = \lambda\tau$. The data for $YbAl_3$ (Fig. 9)[23] clearly show these features. At low temperatures, there is a very marrow Drude peak extending to a deep minimum at 30 meV, above which is a mid IR peak at 150 meV.[24,25] This structure persists up to 40 K, above which it smoothly alters in the direction of normal Drude behavior. (Since the Kondo temperature is of order 600 K in this compound, normal Drude behavior should not be recovered until very high temperatures.)

The IV compound $CePd_3$ shows similar features: a very narrow Drude resonance separated by a very deep minimum in the conductivity from a mid-IR peak. The data for $CePd_3$ were analyzed under the assumption of a frequency-dependent scattering rate:

$$\sigma(\omega) = (ne^2/m_b)[\gamma(\omega) - i\omega]^{-1} \tag{7}$$

where $\lambda(\omega) = -\mathrm{Im}\,\gamma(\omega)/\omega$ and so the mass enhancement $m^* = \lambda m_b$ is both frequency and temperature dependent. This analysis gave mass enhancements of order $\lambda = 40$ for $CePd_3$ at low temperature. For $YbAl_3$ this procedure gives $m^* \sim 25$–30 m_e, comparable to the masses observed in the dHvA measurement.

Recent work[26,27] on a number of IV compounds has shown that the energy $E_{\text{mid-IR}}$ of the mid-IR peak can be related to the hybridization as expected for the

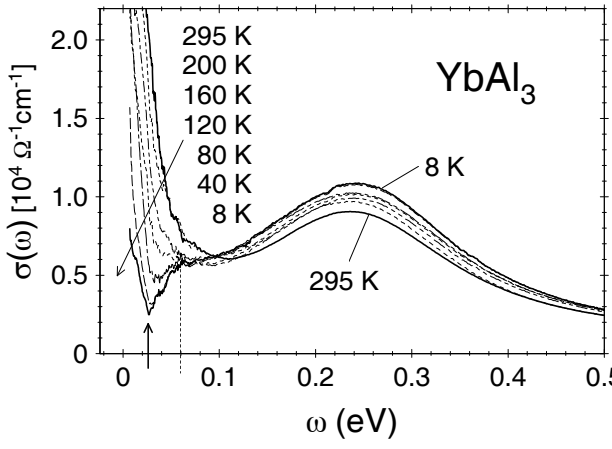

Fig. 9. The optical conductivity of $YbAl_3$ for temperatures in the range 7–295 K. Below $T_{coh} = 40$ K, the mid-infrared feature centered near 150 meV, which is believed to represent optical ($Q = 0$) transitions across the hybridization gap (see Fig. 8), is invariant, so that the coherent hybridized bands are well-established below this temperature. Note the deep minimum near 30 meV, separating the mid-IR peak from a very narrow Drude resonance at low temperatures, as well as the overall renormalization of the spectrum towards broad Drude scattering at very high temperature. (Adapted with permission from Ref. 23, Copyright 2004, Physical Society of Japan.)

Anderson lattice:

$$E_{\text{mid-IR}} = 2\tilde{V} \sim \sqrt{(T_K W)} \tag{8}$$

where the bandwidth W is inversely proportional to the density of states and the latter formula is based on Eq. (4). By determining T_K and W from the specific heat coefficients of the Ce (Yb) and nonmagnetic counterpart La (Lu) compounds, and correctly accounting for orbital degeneracy, good agreement is found for $E_{\text{mid-IR}}$ for such diverse IV compounds as $YbAl_3$, $YbInCu_4$, $YbAgCu_4$, $CeSn_3$ and $CePd_3$. This demonstrates graphically that the scale of the hybridization gap is the renormalized hybridization $\tilde{V}$.

Two further comments are in order. First, as can be seen from Fig. 9, the development of renormalized Drude behavior with decreasing temperature is connected with a transfer of spectral weight over large (eV) energy scales but over much smaller temperature scales. Such transfer is endemic in excited state spectroscopies of correlated electron materials.[28] Second, the fact that the renormalization seen in the optical conductivity of $YbAl_3$ is complete below 40 K allows us to identify this temperature as the "coherence temperature." In confirmation of this identification, we point to the fact that the Fermi liquid T^2 behavior of the resistivity is valid in precisely the same temperature range $0 < T < 40$ K. This is quite significant, because the meaning of "coherence temperature" is often unclear, especially in the truly heavy Fermion compounds, where AF correlations strongly affect the ground state.

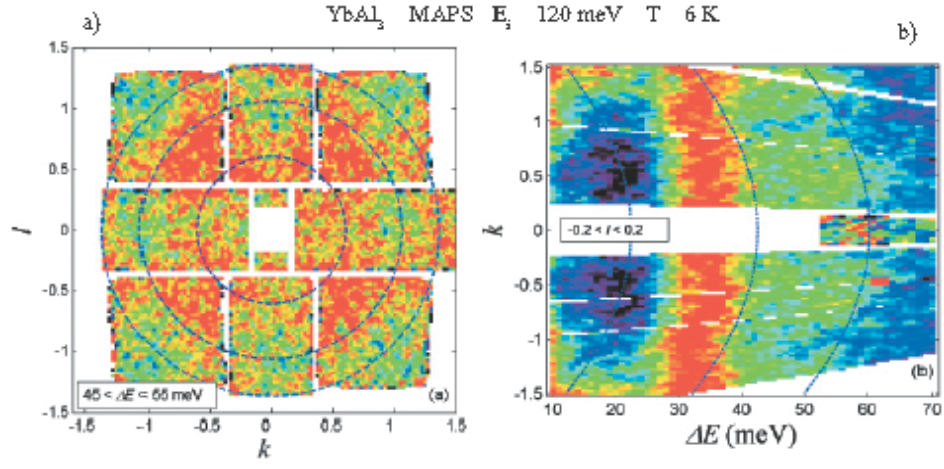

Fig. 10. (a) Neutron scattering intensity versus reduced wavevector (k, l) for energy transfers in the range $40 < \Delta E < 56$ meV for $YbAl_3$ at 6 K. Maximum intensity is at the $k = 0.5$, $l = 0.5$ zone boundary. (b) Intensity versus energy transfer ΔE and reduced wavevector k for the component ℓ of reduced wavevector in the range $-0.2 < \ell < 0.2$. (Data taken on the MAPS spectrometer at ISIS, Rutherford–Appleton Laboratory. Adapted with permission from Ref. 31, Copyright 2006, American Physical Society.)

Neutron scattering is also affected by the hybridization gap. The cross section at fixed momentum and energy transfer is proportional to a convolution over the initial and final states for the given $\mathbf{Q}$ and ΔE. Two peaks, from interband scattering across the gap and from intraband Drude-like scattering near the Fermi energy, are expected.[29] For the interband excitations, there should be a threshold at the energy of the indirect gap, which as mentioned is the Kondo Energy. For smaller $\mathbf{Q}$, the intergap spectrum should be more like the optical conductivity ($\mathbf{Q} = 0$), i.e. peaking on the larger scale $\tilde{V}$ of the direct gap. Since the joint density of initial and final states should be biggest for zone boundary $\mathbf{Q_{BZ}}$ which connects two regions of large $4f$ DOS (see Fig. 8) the intensity should be biggest for threshold scattering at $\mathbf{Q_{BZ}}$. For the intraband transitions, the spin dynamics should exhibit Fermi liquid scattering[30] across ε_F, characterized by an energy scale that varies linearly in $\mathbf{Q}$: $\Gamma \sim v_F\ \mathbf{Q}$. (This form of scattering has never been observed in any IV metal.)

For $YbAl_3$, the Q-resolved low temperature magnetic scattering shows[31] two features (Fig. 2(a)): a broad feature near $E_1 = 50$ meV, which energy is essentially $k_B T_K$ (and hence should be the indirect gap energy), and a narrow feature near $E_2 = 30$ meV, the energy of the deep minimum in the optical conductivity. In Fig. 10(b) we show the intensity for $YbAl_3$ at $Q_L = 0$ as a function of Q_K and ΔE. The band of constant color near $E_2 = 32$ meV means that the E_2 excitation is independent of Q along the Q_K direction. Such an excitation is not an expected feature of the Anderson lattice, and will be discussed further below. In Fig. 10(a) we show the scattering intensity at energy transfer $E_1 = 50$ meV at various positions in the Q_K, Q_L scattering plane. The peak intensity occurs near $(Q_K, Q_L) = (1/2, 1/2)$,

i.e. at the zone boundary. An identical intensity modulation has been observed[32] for $CePd_3$, where the intergap excitation peaks at $k_BT_K = 60$ meV. Such a Q-dependence on the Kondo scale is as expected for intergap transitions in the Anderson lattice, and gives additional evidence for the hybridization gap concept. A caveat is that the intensity at the indirect gap energy at small Q is much larger than expected based on the model, where it is expected to vanish. This may be explained by the effects of real band structure (as opposed to the idealized model of Fig. 8), or by many-body effects which broaden the scattering; furthermore, the Fermi liquid scattering may be sufficiently broad in energy to overlap the threshold.

We thus see that the dHvA experiments validate the band theoretic approach to understanding IV metals, although underestimating the effective masses. The optical conductivity and neutron scattering experiments appear to validate significant aspects of the Anderson lattice approach, yielding both evidence for the hybridization gap and enhanced effective masses, but (at present) not giving detailed information on the topology of the Fermi surface. Overall, we have a good qualitative understanding; quantitative agreement will require combination of the two approaches, e.g. by supplementing the band theory with many-body treatment of the correlations. For example, the enhanced effective masses observed in the dHvA experiments on $CeSn_3$ have been reproduced by the LDA + U method.[33]

We showed above that experimental quantities such as the specific heat, susceptibility, valence and Q-averaged spin dynamics are qualitatively in good accord with the predictions of the AIM over a broad range of temperature, reflecting the highly localized spin/valence fluctuations. Nevertheless, recent theory[34,35] for the Anderson Lattice suggests that the behavior of these latter quantities can differ in two ways from the predictions of the AIM. First, the evolution with temperature from Fermi liquid to local moment behavior can proceed more slowly than predicted by the AIM. We have termed this effect "slow crossover."[8] Second, there can be a non-universal low temperature scale for coherence, with associated low temperature anomalies (relative the AIM) in the given measurements. In both cases, theory[34,35] predicts that these differences become magnified when the conduction electron or hole density is low, or when there is significant structure in the background DOS near the Fermi level.

Slow crossover has been observed[8] in the series $YbXCu_4$, where it has been correlated to the electron density $n_e = 1/R_He$ determined from the Hall coefficient. In particular, for YbAgCu4 and $YbTlCu_4$, the density is large ($n_e > 1e$/atom) and the data fit the AIM (Fig. 3). Slow crossover occurs for $YbMgCu_4$ and $YbZnCu_4$ where $n_e < 1e$/atom. Slow crossover can also be observed for $YbAl_3$ (Fig. 1) where $n_e = 1/R_He = 0.5e$/atom. To a great extent, this effect reflects the fact that the evolution of the valence (e.g. Fig. 1(c)) in the Anderson lattice involves one degree of freedom *per atom*, and hence the change of valence ($z = 2 + n_f$ for Yb) requires a significant change in the kinetic energy, which retards the transition. This does

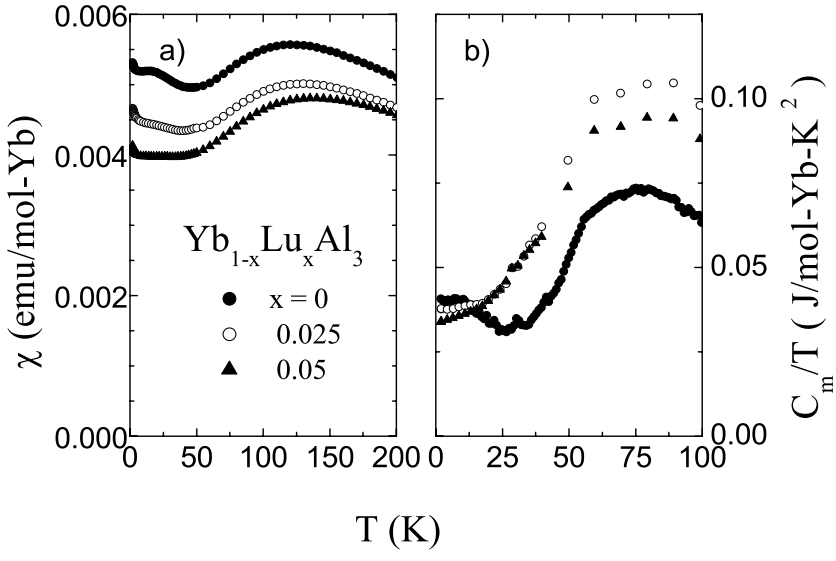

Fig. 11. (a) Susceptibility χ and (b) magnetic specific heat coefficient C_m/T of $Yb_{1-x}Lu_xAl_3$ alloys. The low temperature anomalies observed in $YbAl_3$ are absent for $x = 0.05$. (Adapted with permission from Ref. 39, Copyright 2003, American Physical Society.)

not occur in the AIM where only one degree of freedom for the single impurity is involved.

While the behavior of such IV compounds as $YbAgCu_4$ agrees well with the AIM, low temperature anomalies can be observed in other IV compounds. Apart from slow crossover, the susceptibility and specific heat of $YbAl_3$ correspond qualitatively to the predictions of the AIM for $T > 40$ K, but both quantities exhibit a low temperature maximum over and beyond the predictions of the AIM (Fig. 1). These anomalies occur only in the cleanest samples, are destroyed rapidly by alloying (Fig. 11),[36] and occur on the same temperature scale T_{coh} as the fully renormalized optical conductivity and the Fermi liquid T^2 resistivity (Figs. 5 and 9). These facts indicate the importance of lattice coherence in the occurrence of the anomalies. Two peaks in the susceptibility are predicted by several approximate treatments of the Anderson lattice;[29,35,37,38] the extra low temperature peak reflects the low energy Fermi liquid excitations discussed above for the neutron scattering. As mentioned, extra peaks are associated in the theory with low conduction density; hence their observation in $YbAl_3$ ($n \sim 0.5$) and $CePd_3$ (where $n \sim 0.1$) may well be expected signatures of the Anderson lattice.

That the anomalies are associated with a change in Fermi surface is implied by high field dHvA which shows[39] (Fig. 12) that the effective masses for $H//\langle 111\rangle$ decrease substantially for $H > 40$ T. This field is much smaller than the Kondo field $B_K = kT_K/gJ\mu_B$ required to polarize the f electrons, but is of order k_BT_{coh}/μ_B. A field of this magnitude also suppresses the low temperature susceptibility anomaly

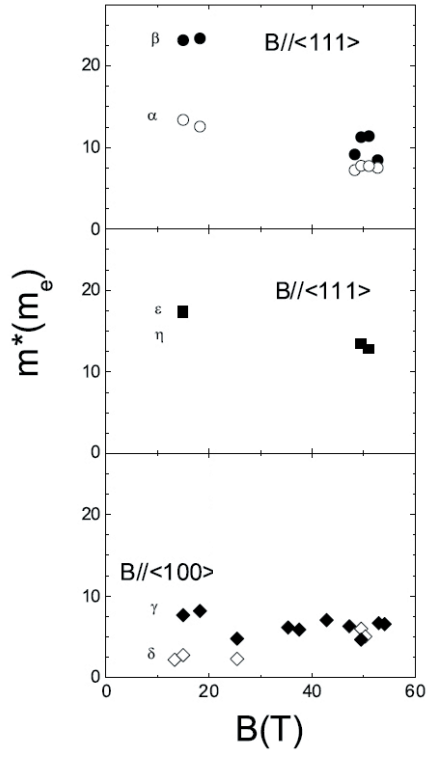

Fig. 12. Effective masses for various branches (see Fig. 7 for the notation) measured by dHvA for $YbAl_3$ versus magnetic field. A transition towards a lower mass state occurs near 40 T. (Reprinted with permission from Ref. 39, Copyright 2003, American Physical Society.)

(Fig. 13). It is as though the system exhibits a crossover from an anomalous high mass Fermi Liquid state to a non-anomalous moderately enhanced Fermi liquid state for $\mu_B H > k_B T_{coh}$.

Finally, we consider the new peak in the low temperature spin dynamics at $E_2 = 32$ meV (Fig. 2(b)). This peak vanishes above 50 K, and hence appears to be yet another "anomalous" property of the fully coherent ground state of $YbAl_3$. The lack of Q-dependence of this peak (Fig. 10(b)) is highly unusual. Such behavior has not been observed in any other IV compound to date. The Q-independent peak at 30 meV in $YbAl_3$ is suggestive of the existence of a localized magnetic exciton whose energy is in the middle of the hybridization gap. Such a local state is not expected for the Anderson lattice, and hence is truly anomalous.

A low temperature susceptibility anomaly also occurs[40] in $CePd_3$. In that compound it is clearly associated with an anomaly in the neutron form factor,[41,42] which measures the spatial distribution of magnetization around the Ce site. At high T the form factor has the same Q (or r) dependence $f^2(4f;Q)$ as the $4f$ radial function (solid line in Fig. 14). At low temperature, a more diffuse $5d$ component $f^2(5d;Q)$ is

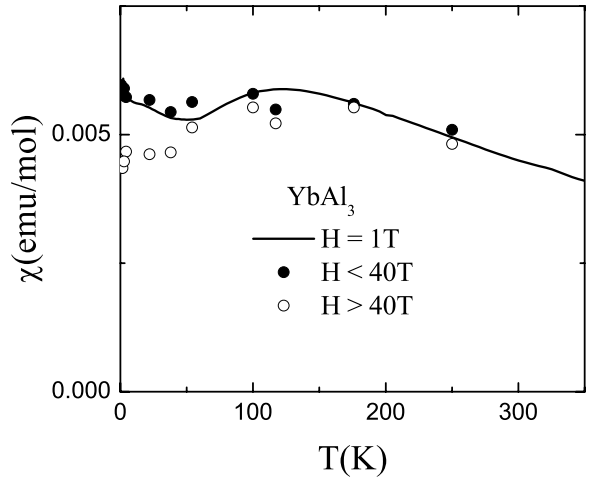

Fig. 13. Susceptibility of $YbAl_3$ at low and high magnetic field. The susceptibility anomaly is suppressed for fields above 40 T. (Adapted with permission from Ref. 39, Copyright 2003, American Physical Society.)

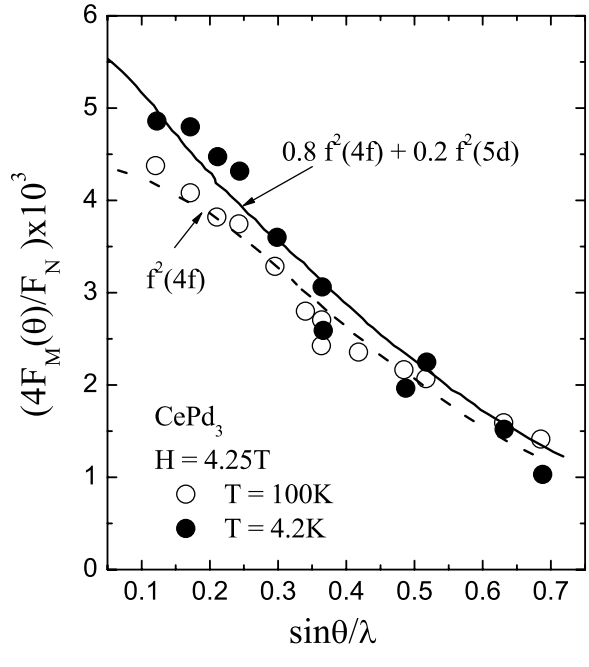

Fig. 14. Paramagnetic form factor of $CePd_3$ measured at 100 K (open circles) and 4.2 K (closed circles). The data at 100 K are well-fit by the predicted $4f$ form factor (dashed line), but at 4.2 K, an additional small-Q (spatially diffuse) component is observed. The fit at low temperature (solid line) assumes 80% $4f$ and 20% $5d$ contributions. (Adapted with permission from Ref. 41, Copyright 1982, American Institute of Physics.)

present $f^2(Q) = a^2 f^2(4f) + (1-a^2) f^2(5d)$ (dashed line). The $5d$ contribution gives rise to an anomalous increase in the low temperature ($T < 50$ K) susceptibility over and beyond the peak near 150 K predicted by the AIM. Such an increase of $5d$ susceptibility on such a small temperature scale is quite unusual; it must reflect the coherent hybridization that occurs in the hybridized ground state. We note, however, that in $YbAl_3$, there is no form factor anomaly[43] — the magnetization density is that of the $4f$ orbital at all temperatures. Hence the effect, and its role in the susceptibility anomaly, is not universal.

We can summarize the behavior of IV metals as follows. The Kondo temperature (typically $T_K \sim 500$ K) sets the main scale for the crossover from local moment behavior to nonmagnetic behavior. At high T the behavior is that of uncorrelated Kondo impurities, and properties such as the susceptibility, specific heat, temperature-dependent valence and Q-integrated neutron scattering line shape, which are dominated by highly localized spin fluctuations, fit qualitatively and sometimes quantitatively to the Anderson impurity model (AIM). A major disagreement with the AIM at these temperatures, the slow crossover from the low temperature Fermi liquid behavior to the high temperature local moment state, may be a consequence of low electron or hole density.

Properties that are highly sensitive to lattice order – d.c. transport (resistivity), optical conductivity, de Haas van Alphen – require treatment of the lattice periodicity. Below a low temperature scale for the onset of coherence ($T_{coh} \sim 50$ K) the following occurs: T^2 behavior of the resistivity; rapid change in the Hall coefficient indicating a change in carrier density; large effective masses on an otherwise LDA Fermi surface observed in dHvA; fully developed hybridization gap and renormalized Drude mass in the optical conductivity; and a Q-dependent inelastic neutron scattering on the scale of the Kondo energy, peaking in intensity at the zone boundary, reflecting indirect transitions across the hybridization gap. Low energy scattering with a Q-dependence characteristic of a Fermi liquid should in principle also be observed. These properties can all be understood qualitatively based on a combination of band theory and correlated electron many-body theory, i.e. the Anderson lattice. Band theory gets the shape of the Fermi surface correctly, but cannot get the large mass enhancements or the temperature dependence. Anderson lattice theory gets the mass enhancements and the temperature dependence but forsakes the Fermi surface geometry. It predicts key features of the optical conductivity and the neutron scattering, in particular that there will be a hybridization gap, with intergap transitions strong for momentum transfer Q at the zone boundary.

In addition, "anomalies" occur in some, but not all, compounds in the low temperature state. These include new peaks in susceptibility and specific heat, new peaks in the spin dynamics, and $5d$ contributions to the rare earth form factor. These features are not universal, but specific to given compounds, and may reflect details of the band structure, electron density, etc.

Future improvement in our understanding of IV metals will require advances both in theory and experiment. The advent of the combination of LDA and dynamic mean field theory[44] is a very promising theoretical development, giving hope for realistic band calculations that correctly embody the strong local correlations. The resulting band structures can then be used for better agreement with the masses measured by dHvA and for more realistic calculations of the optical conductivity and neutron scattering than can be obtained from schematic band structure such as Fig. 8. Recent advances in photoemission give hope for detailed Fermi surface maps, on the small (meV) energy scales of the expected $4f$ dispersion. Improvements in crystal quality will be necessary for dHvA experiments in such compounds as $CePd_3$, $YbAgCu_4$, etc. Neutron scattering experiments need to be extended to a broader range of momentum and energy transfers, especially the low energy region where excitations characteristic of a Fermi liquid are expected but have not been seen. Hopefully, newer techniques, such as STM, will be applied to obtain deeper understanding of these materials. These efforts will be very worthwhile, in that a deep understanding of the correlated electron physics of IV metals will have important implications not only for heavy Fermion compounds, with which they have so much in common, but for correlated electron materials much more generally.

Acknowledgments

The ideas in this paper have emerged from ongoing discussions with many fellow researchers. I would like to particularly thank my senior collaborators Joe Thompson, Zachary Fisk and Peter Riseborough. Work at Irvine was supported by the U.S. Department of Energy under Grant No. DE-FG03-03ER46036.

References

1. J. M. Lawrence, P. S. Riseborough and R. D. Parks, *Rep. Prog Phys.* **44** (1981) 1.
2. J. M. Lawrence, in *Encyclopedia of Physics*, 3rd edn., eds. R. G. Lerner and G. L. Trigg (Wiley-VCH, Berlin, 2005), p. 1114.
3. P. Wachter, in *Handbook on the Physics and Chemistry of the Rare Earths*, Vol. 19, ed. K. A. Gschneidner Jr. *et al.* (Elsevier Science B.V., Amsterdam, 1994), p. 177.
4. N. Grewe and F. Steglich, in *Handbook on the Physics and Chemistry of the Rare Earths*, Vol. 14, eds. K. A. Gschneidner Jr. and L. Eyring (Elsevier Science B.V., Amsterdam, 1991), p. 343.
5. H. V. Löhneysen, A. Rosch, M. Votja and P. Wölfle, *Rev. Mod. Phys.* **79** (2007) 1015.
6. P. S. Riseborough, *Adv. Phys.* **49** (2000) 257.
7. A. L. Cornelius, J. M. Lawrence, T. Ebihara, P. S. Riseborough, C. H. Booth, M. F. Hundley, P. G. Pagliuso, J. L. Sarrao, J. D. Thompson, M. H. Jung, A. H. Lacerda and G. H. Kwei, *Phys. Rev. Lett.* **88** (2002) 117201.
8. J. M. Lawrence, P. S. Riseborough, C. H. Booth, J. L. Sarrao, J. D. Thompson and R. Osborn, *Phys. Rev. B* **63** (2001) 054427.
9. E. Holland-Moritz and G. H. Lander, in *Handbook on the Physics and Chemistry of the Rare Earths*, Vol. 19, eds. K. A. Gschneidner Jr. *et al.* (Elsevier Science B.V., Amsterdam, 1994) p. 1.

10. J. M. Lawrence, S. M. Shapiro, J. L. Sarrao and Z. Fisk, *Phys. Rev. B* **55** (1997) 14467.
11. A. C. Hewson, *The Kondo Problem to Heavy Fermions* (Cambridge University Press, Cambridge, UK, 1993).
12. T. Kasuya and T. Sato (eds.), *Theory of Heavy Fermions and Valence Fluctuations* (Springer-Verlag, Berlin, 1985).
13. J. M. Lawrence, A. J. Arko, J. J. Joyce, R. I. R. Blyth, R. J. Bartlett, P. C. Canfield, Z. Fisk and P. S. Riseborough, *Phys. Rev. B* **47** (1993) 15460.
14. A. J. Arko, P. S. Riseborough, A. B. Andrews, J. J. Joyce, A. N. Tahvildar-Zadeh and M. Jarrell, in *Handbook on the Physics and Chemistry of the Rare Earths*, Vol. **26**, eds. K. A. Gschneidner Jr. and L. Eyring (Elsevier Science B.V., Amsterdam, 1999), p. 265.
15. J. W. Allen, in *Synchrotron Radiation Research*, Vol. 1, ed. R. Z. Bachrach (Plenum, New York, 1992), p. 253.
16. M. Garnier, K. Breuer, D. Purdie, M. Hengsberger, Y. Baer and B. Delley, *Phys. Rev. Lett.* **78** (1997) 4127.
17. N. Tsujii, H. Kontani and Y. Yoshimura, *Phys. Rev. Lett.* **94** (2005) 057201.
18. E. Cattaneo, *Zeit. Physik B* **64** (1986) 305; 317.
19. J. D. Denliger, G.-H. Gweon, J. W. Allen, C. G. Olsen, Y. Dalichaouch, B.-W. Lee, M. B. Maple, Z. Fisk, P. C. Canfield and P. E. Armstrong, *Physica B* **281–282** (2000) 716.
20. T. Ebihara, Y. Inada, M. Murakawa, S. Uji, C. Terakura, T. Terashima, E. Yamamoto, Y. Haga, Y. Ōnuki and H. Harima, *J. Phys. Soc. Jpn.* **69** (2000) 895.
21. Y. Ōnuki and A. Hasegawa, *J. Magn. Mag. Mat.* **108** (1992) 19.
22. R. M. Martin and J. W. Allen, in *Valence Fluctuations in Solids*, eds. L. M. Falicov *et al.* (North Holland, Amsterdam, 1981), p. 85.
23. H. Okamura, T. Michizawa, T. Nanba and T. Ebihara, *J. Phys. Soc. Jpn.* **73** (2004) 2045.
24. B. C. Webb, A. J. Sievers, T. Mihalisin, *Phys. Rev. Lett.* **57** (1986) 1951.
25. B. Bucher, Z. Schlesinger, D. Mandrus, Z. Fisk, J. Sarrao, J. F. DiTusa, C. Oglesby, G. Aeppli and E. Bucher, *Phys. Rev. B* **53** (1996) R2948.
26. J. N. Hancock, T. McKnew, Z. Schlesinger, J. L. Sarrao and Z. Fisk, *Phys. Rev. Lett.* **92** (2004) 186405.
27. H. Okamura, T. Watanabe, M. Matsunami, T. Nishihara, N. Tsujii, T. Ebihara, H. Sugawara, H. Sato, Y. Ōnuki, Y. Isikawa, T. Takabatake and T. Nanba, *J. Phys. Soc. Jpn.* **76** (2007) 023703.
28. M. J. Rozenburg, G. Kotliar and H. Kajueter, *Phys. Rev. B* **54** (1996) 8452.
29. A. A. Aligia and B. Alascio, *J. Magn. Mag. Mat.* **46** (1985) 321.
30. N. R. Bernhoeft and G. G. Lonzarich, *J. Phys: Condens. Matt.* **7** (1995) 7325.
31. A. D. Christianson, V. R. Fanelli, J. M. Lawrence, E. A. Goremychkin, R. Osborn, E. D. Bauer, J. L. Sarrao, J. D. Thompson, C. D. Frost and J. L. Zarestky, *Phys. Rev. Lett.* **96** (2006) 117206.
32. J. M. Lawrence, V. R. Fanelli, E. A. Goremychkin, R. Osborn, E. D. Bauer, K. J. McClellan and A. D. Christianson, *Physica B* **403** (2008) 783.
33. S. Tanaka, H. Harima and A. Yanase, *J. Magn. Mag. Mat.* **177–181** (1998) 329.
34. A. N. Tahvildar-Zadah, M. Jarrell and J. K. Freericks, *Phys. Rev. B* **55** (1997) R3332; *Phys. Rev. Lett.* **80** (1998) 5168.
35. S. Burdin, A. Georges and D. R. Gempel, *Phys. Rev. Lett.* **85** (2000) 1048.
36. E. D. Bauer, C. H. Booth, J. M. Lawrence, M. F. Hundley, J. L. Sarrao, J. D. Thompson, P. S. Riseborough and T. Ebihara, *Phys. Rev. B* **69** (2004) 125102.

37. B. Brandow, *Phys. Rev. B* **37** (1988) 250.
38. Y. Ono, T. Matsuura and Y. Kuroda, *J. Phys. Soc. Jpn.* **60** (1991) 3475.
39. T. Ebihara, E. D. Bauer, A. L. Cornelius, J. M. Lawrence, N. Harrison, J. D. Thompson, J. L. Sarrao, M. F. Hundley and S. Uji, *Phys. Rev. Lett.* **90** (2003) 166404.
40. J. R. Thompson, S. T. Seulas, C.-K. Loong and C. Stassis, *J. Appl. Phys.* **53** (1982) 7893.
41. C. Stassis, C.-K. Loong, J. Zarestky, O. D. McMasters, R. M. Moon and J. R. Thompson, *J. Appl. Phys.* **53** (1982) 7890.
42. F. Givord, R. M. Galéra, A. P. Murani and E. Lelièvre-Berna, *Physica B* **350** (2004) e103.
43. A. Hiess, J. X. Boucherle, F. Givord, J. Schweizer, E. Lelièvre-Berna, F. Tasset, B. Gillon and P. C. Canfield, *J. Phys.: Cond. Matt.* **12** (2000) 829.
44. K. Held, I. A. Nekrasov, G. Keller, V. Eyert, N. Blümer, A. K. McMahan, R. T. Scalettar, Th. Pruschke, V. I. Anisimov and D. Vollhardt, *Phys. Stat. Sol. B* **243** (2006) 2599.